

1 **Exergoeconomic Analysis of an Absorption Refrigeration and Natural**  
2  
3  
4 **Gas-Fueled Diesel Power Generator Cogeneration System**

5  
6  
7  
8  
9  
10 **4 Felipe Raúl Ponce Arrieta\***

11  
12 Pontifical Catholic University of Minas Gerais, Department of Mechanical Engineering

13  
14  
15 Av. Dom José Gaspar, 500 - 30535-901 – Belo Horizonte – MG - Brazil

16  
17 Phone: +55-31-9614-5380 - Fax: +55-31-3319-4910 - E-mail: felipe.ponce@pucminas.br

18  
19  
20  
21 **8 José Ricardo Sodré**

22  
23 Pontifical Catholic University of Minas Gerais, Department of Mechanical Engineering

24  
25  
26 Av. Dom José Gaspar, 500 - 30535-901 – Belo Horizonte – MG - Brazil

27  
28 Phone: +55-31-3319-4911 - Fax: +55-31-3319-4910 - E-mail: ricardo@pucminas.br

29  
30  
31 **12 Mario David Mateus Herrera**

32  
33 Pontifical Catholic University of Minas Gerais, Department of Mechanical Engineering

34  
35  
36 Av. Dom José Gaspar, 500 - 30535-901 – Belo Horizonte – MG - Brazil

37  
38  
39 Phone: +55-31-3319-4910 - E-mail: mario\_mateus\_h@hotmail.com

40  
41  
42 **16 Paola Helena Barros Zárante**

43  
44 Pontifical Catholic University of Minas Gerais, Department of Mechanical Engineering

45  
46  
47 Av. Dom José Gaspar, 500 - 30535-901 – Belo Horizonte – MG - Brazil

48  
49 Phone: +55-31-9670-0290 - E-mail: paolabarros@hotmail.com

50  
51  
52  
53 **20 \* corresponding author**

1 21 **ABSTRACT**

2  
3 22

4  
5  
6 23 This work presents a thermoeconomic analysis of a cogeneration system using  
7  
8 24 the exhaust gas from a natural gas-fueled diesel power generator as heat source for an  
9  
10  
11 25 ammonia-water absorption refrigeration system. The purpose of the analysis is to obtain  
12  
13 26 both unit exergetic and exergoeconomic costs of the cogeneration system at different  
14  
15  
16 27 load conditions and replacement rates of diesel oil by natural gas. A thermodynamic  
17  
18 28 model of the absorption chiller was developed using the Engineering Equation Solver  
19  
20 29 (EES) software to simulate the exergetic and exergoeconomic cogeneration costs. The  
21  
22 30 data entry for the simulation model included available experimental data from a dual-  
23  
24  
25 31 fuel diesel power generator operating with replacement rates of diesel oil by natural gas  
26  
27  
28 32 of 25%, 50% and 75%, and varying engine load from 10 kW to 30 kW. Other required  
29  
30 33 data was calculations using the GateCycle software, from the available experimental  
31  
32  
33 34 data. The results show that, in general, the cogeneration cold unit exergetic and  
34  
35 35 exergoeconomic costs increases with increasing engine load and decreases with  
36  
37  
38 36 increasing replacement rate of diesel oil by natural gas under the conditions  
39  
40 37 investigated. Operating with 3/4 of the rated engine power and replacing 50% of diesel  
41  
42 38 oil by natural gas, the exergoeconomic cost of the produced power is increased by 75%,  
43  
44  
45 39 and the exergoeconomic cost of the produced cold is decreased by 17%. The electric  
46  
47 40 power unit exergetic and exergoeconomic costs indicate that the replacement of diesel  
48  
49  
50 41 oil by natural gas is feasible in the present considerations for engine operation at  
51  
52 42 medium and high loads.

53  
54  
55 43  
56  
57  
58  
59  
60

1 44 Keywords: natural gas; cogeneration; absorption refrigeration; power generation;  
2  
3 45 exergoeconomic analysis.  
4  
5  
6  
7  
8  
9  
10  
11  
12  
13  
14  
15  
16  
17  
18  
19  
20  
21  
22  
23  
24  
25  
26  
27  
28  
29  
30  
31  
32  
33  
34  
35  
36  
37  
38  
39  
40  
41  
42  
43  
44  
45  
46  
47  
48  
49  
50  
51  
52  
53  
54  
55  
56  
57  
58  
59  
60  
61  
62  
63  
64  
65

1 46 **1. INTRODUCTION**

2  
3 47

4  
5  
6 48 Absorption cycles have emerged as promising alternatives for cooling and  
7  
8 49 refrigeration applications in terms of emissions (zero ozone depletion fluids and zero  
9  
10  
11 50 global warming fluids) and low electric energy consumption [1]. Absorption  
12  
13 51 refrigeration systems are capable of using different energy sources such as fossil fuels,  
14  
15  
16 52 renewable energies and waste heat from other thermal systems, such as engine exhaust  
17  
18 53 gas. Diesel engines deliver high amounts of easily recovered waste heat energy, but  
19  
20 54 requires single-effect absorption cycles to operate with low activation temperatures once  
21  
22  
23 55 the exhaust gas temperature is low [1].  
24

25 56 Several authors [2-5] studied cogeneration plants with reciprocating engines. An  
26  
27  
28 57 absorption refrigeration system using waste heat from a 55-passenger bus engine could  
29  
30 58 completely meet the coach cooling demand of 30 kW when the vehicle operated over  
31  
32  
33 59 100 km/h [6]. A simulation analysis of an absorption refrigeration unit operating with  
34  
35 60 the exhaust gas from a diesel engine showed that the overall system performance could  
36  
37  
38 61 be improved with precooling of the engine intake air charge to increase the pressure  
39  
40 62 ratio, while maintaining low cycle temperature ratio [7]. A combined effect Lithium-  
41  
42 63 Bromide (LiBr) absorption chiller was shown to have higher coefficient of performance  
43  
44  
45 64 (COP) and cooling capacity than a single effect absorption chiller, both using waste heat  
46  
47 65 from the exhaust gas of an engine as energy source [8].  
48  
49

50 66 The generator is the component of an absorption refrigeration system with the  
51  
52 67 highest exergy destruction, followed by the absorber, condenser and evaporator [9]. It  
53  
54  
55 68 was reported that the generator, evaporator, condenser and absorber temperatures, and  
56  
57 69 the solution concentration affect the absorption refrigeration system COP [10]. In  
58  
59  
60

1 70 another work, it was found that the highest performance of an ammonia-water  
2  
3 71 absorption refrigeration cycle integrated with a marine diesel engine was obtained at  
4  
5  
6 72 high generator and evaporator temperatures, and low condenser and absorber  
7  
8 73 temperatures [11].  
9

10  
11 74 An experimental investigation of a solar thermal powered ammonia-water  
12  
13 75 absorption refrigeration system indicated a chiller COP of 0.69 and cooling capacity of 10.1  
14  
15  
16 76 kW, with generator inlet temperature of 114°C, condenser/absorber inlet temperature of  
17  
18 77 23°C, and evaporator outlet temperature of -2°C [12]. A hybrid absorption-compression  
19  
20 78 refrigeration powered by mid-temperature waste heat reached a COP of 0.71, which is  
21  
22  
23 79 about 42% higher than that of a conventional ammonia-water absorption refrigeration  
24  
25 80 system [13]. An energetic and exergetic study of a 10 RT (35.17 kW), single effect, indirect  
26  
27  
28 81 heated LiBr absorption chiller coupled to a 30 kW microturbine, cooling tower and a heat  
29  
30 82 exchanger, using the Engineering Equation Solver (EES) software to evaluate the influence  
31  
32  
33 83 of the system parameters, reports a COP around 0.7 for microturbine operation between  
34  
35 84 80% and 100% of the rated load [14]. The COP of a double effect LiBr absorption chiller,  
36  
37  
38 85 of 1.411, was higher than that of a single effect chiller, of 0.809, both operating with waste  
39  
40 86 heat recovery from a boiler flue gas [15]. The exergetic efficiency of the absorption systems  
41  
42 87 decreased with increasing flue gas temperature due to the rise of irreversibility in the low  
43  
44  
45 88 pressure generator.  
46

47 89 A thermoeconomic evaluation is important to improve absorption refrigeration  
48  
49  
50 90 systems, as they are less efficient than vapor compression systems [16,17]. An  
51  
52 91 exergoeconomic analysis was performed for three classes of double-effect, lithium  
53  
54  
55 92 bromide-water absorption refrigeration systems, showing that lower investment costs  
56  
57 93 are attained when the temperatures of the high-pressure generator and the evaporator are  
58

1 94 high, the condenser temperature is low [16]. The exergoeconomic analysis of series flow  
2  
3 95 double effect and combined ejector-double effect lithium bromide-water absorption  
4  
5  
6 96 refrigeration systems pointed out that, with similar operating conditions, the overall  
7  
8 97 system investment cost and the product cost flow rate are lower for the combined cycle  
9  
10  
11 98 [17]. In another work, an exergoeconomic analysis of a 5 kW ammonia-water  
12  
13 99 refrigeration cycle with hybrid storage system, with the solution properties determined  
14  
15  
16 100 by the EES software, showed that the system overall exergetic efficiency tends to a  
17  
18 101 constant at temperatures higher than 120°C, and decreases with evaporator temperature  
19  
20 102 lower than -15°C [18]. A thermoeconomic analysis performed for an absorption  
21  
22  
23 103 refrigeration system using the exhaust gas of a hydrogen-fueled diesel engine as energy  
24  
25 104 source showed that engine combustion is the process with the highest exergy  
26  
27  
28 105 destruction, and that it is feasible to operate the system at intermediate and high engine  
29  
30 106 loads [19].

31  
32  
33 107 This work presents a thermoeconomic analysis of a cogeneration system  
34  
35 108 consisted by a direct heated, single effect, ammonia-water absorption refrigeration  
36  
37  
38 109 system using as heat source the exhaust gas from a diesel power generator fueled by  
39  
40 110 diesel oil and natural gas. The exergetic and exergoeconomic analysis uses a similar  
41  
42 111 approach as that applied by [19]. The main aim is to study the performance parameters  
43  
44  
45 112 of the cogeneration system and to get both exergetic and exergoeconomic costs of  
46  
47 113 power and cold production at different engine load conditions and replacement rates of  
48  
49  
50 114 diesel oil by natural gas. The absorption refrigeration system was modeled in the EES  
51  
52 115 software, using as input data the experimental data available from a production,  
53  
54  
55 116 stationary diesel engine operating in dual fuel mode with replacement rates of diesel oil  
56  
57 117 by natural gas of 25%, 50% and 75%, under variable load [20]. The experimental data  
58

1 118 available was also used by the GateCycle software to calculate unmeasured exhaust gas  
2  
3 119 properties required by the absorption chiller simulation model.  
4  
5

6 120 Natural gas has clean burn features and produces lower levels of most pollutant  
7  
8 121 emissions components, compared with gasoline and diesel oil [21-27]. In dual fuel  
9  
10 122 operation with diesel oil, natural gas combustion increases heat release by about 27-  
11  
12 123 30%, compared to operation with diesel oil as a single fuel [28]. This results in reduced  
13  
14 124 specific fuel consumption, especially at high engine load and intake air temperature [21-  
15  
16 125 23,29]. The use of different replacement rates of diesel fuel by natural gas affects  
17  
18 126 combustion duration and exhaust gas temperature and, therefore, the energy available to  
19  
20 127 be used by the absorption refrigeration system [20]. In this work, the replacement rates  
21  
22 128 chosen allows for the analysis of a broad range of engine operation with equal  
23  
24 129 increments of natural gas in the fuel. The investigation of a cogeneration system  
25  
26 130 composed by an absorption refrigeration system and a diesel power generator operating  
27  
28 131 with different replacement rates of diesel oil by natural gas finds no resemblance to  
29  
30 132 previous works [5,9,11,14].  
31  
32  
33  
34  
35  
36  
37

## 38 133

### 39 134 **2. DESCRIPTION OF THE COGENERATION SYSTEM**

#### 40 135

41  
42 136 A schematics of the absorption refrigeration system simulation coupled with the  
43  
44 137 diesel power generator is shown in Fig. 1. The power generation unit features a four-  
45  
46 138 stroke, four-cylinders, naturally aspirated diesel engine, with direct fuel injection and 44  
47  
48 139 kW rated power at 1800 rpm. The engine has a compression ratio of 17:1, 3.922 L total  
49  
50 140 displacement, 120 mm bore and 120 mm stroke. The simulated absorption refrigeration  
51  
52 141 system is direct heating, single effect, with ~17 kW (~ 4.8 TR) of capacity and COP ~  
53  
54  
55  
56  
57  
58

1 142 0.6. The refrigeration system has a generator containing a double rectifying column with  
2  
3 143 a second heat exchanger and a binary mixture as a combination of refrigerant and  
4  
5  
6 144 absorbent. Ammonia is the refrigerant and water is the absorbent.  
7

8 145 A strong liquid solution with a large concentration of ammonia refrigerant leaves  
9  
10  
11 146 the absorber at state 1 and is pumped to the condensing pressure, being preheated in the  
12  
13 147 heat exchanger to reduce heating at state 3 (Fig. 1). The heated strong solution enters  
14  
15  
16 148 into the generator, which produces a weak liquid solution with low concentration of  
17  
18 149 ammonia refrigerant at the bottom, at state 4, and nearly pure ammonia (99.98%) vapor  
19  
20 150 at the top, at state 7. The weak solution enters the heat exchanger and flows through the  
21  
22  
23 151 pressure reducing valve to enter the absorber. The strong solution is sent to the  
24  
25 152 condenser at state 7, then it condenses to sub-cooled liquid at state 8. The liquid enters  
26  
27  
28 153 the heat exchanger to cool at state 9 and, then, it enters the expansion valve. The  
29  
30 154 ammonia leaving the expansion valve at state 10 enters the evaporator, where the liquid  
31  
32  
33 155 phase vaporizes to absorb the refrigerant load in the system. The refrigerant is further  
34  
35 156 heated in the heat exchanger prior to being absorbed in the weak-liquid solution in the  
36  
37  
38 157 absorber at state 12, and, then, it returns to state 1, thus restarting the refrigeration cycle.  
39

40 158

### 41 159 **3. METHODOLOGY**

42 160

43  
44  
45  
46  
47 161 Figure 2 presents the stages used in the methodology of the cogeneration system  
48  
49  
50 162 simulation: processing of the available data from experimental engine testing and  
51  
52 163 calculation of exhaust gas related parameters by the GateCycle software, and simulation  
53  
54  
55 164 of the absorption refrigeration system and exergoeconomic analysis in the EES  
56  
57 165 software. The experimental data and the results from the GateCycle software are used as  
58  
59  
60



1 166 input data for the EES software, and both softwares operate independently. The  
2  
3 167 simulation does not aim to optimize the performance of the combined cogeneration  
4  
5  
6 168 system, but to produce the necessary information for an exergetic and exergoeconomic  
7  
8 169 analysis of system operation with different replacement rates of diesel fuel by natural  
9  
10  
11 170 gas.

12  
13 171 The experimental data was available from tests in a production, four-stroke,  
14  
15  
16 172 four-cylinder, stationary diesel engine, model MWM D229-4, of 44 kW rated power  
17  
18 173 operating at 1800 rev/min, compression ratio 17:1 and direct diesel fuel injection (Tab.  
19  
20 174 1) [29]. For all tested operating conditions, the exhaust gas temperature at the outlet of  
21  
22  
23 175 the refrigeration system generator was  $58^{\circ}\text{C} \pm 6^{\circ}\text{C}$  lower than the inlet gas temperature.  
24  
25 176 The engine was operated with varying load from 10 kW to 30 kW and with replacement  
26  
27  
28 177 rates of diesel oil by natural gas of 0%, 25%, 50% and 75% on energy basis. During the  
29  
30 178 tests, the load power range was limited to 30 kW and the natural gas concentration was  
31  
32  
33 179 limited to 75% due to engine instability to operate with natural gas at higher loads and  
34  
35 180 concentrations without major modifications. Additional details of the tests, including  
36  
37  
38 181 the uncertainties of the results, can be found in Ref [29].

39  
40 182 The GateCycle software uses the experimental data from the engine tests  
41  
42 183 varying the load applied and the replacement rate of diesel fuel by natural gas (Tab. 1)  
43  
44  
45 184 to calculate unmeasured parameters by bivariate interpolation. The motivation to use the  
46  
47 185 GateCycle software was the possibility to use its internal libraries and adequately  
48  
49  
50 186 estimate the exhaust gas properties required by the simulation model of the absorption  
51  
52 187 refrigeration system.

53  
54  
55 188 The compositions of natural gas and diesel oil are presented in Table 2. For  
56  
57 189 calculation of the total exergy of air, exhaust gas, diesel oil and natural gas, it was  
58

1 190 considered steady state condition, negligible pressure drop and ambient at 30°C, 101.32  
2  
3 191 kPa [20]. The exergetic efficiency of the diesel power generator ( ) is calculated by [19]:  
4  
5

6 192  
7  
8  
9  
10  
11  
12  
13 193  
14  
15 194 Where is the output power from the diesel power generator (kW), is  
16  
17  
18 195 the total exergy supplied with the fuel (kW), is the diesel oil mass flow rate  
19  
20 196 (kg/s), is the natural gas mass flow rate (kg/s), is the diesel oil specific exergy  
21  
22  
23 197 (Table 2) (kJ/kg), and is the natural gas specific exergy (Table 2) (kJ/kg).  
24

25 198 The simulation model of the absorption refrigeration system, developed in the  
26  
27  
28 199 EES software, was validated against experimental data available from a commercial,  
29  
30 200 Consul CQG22D model ammonia-water absorption refrigerator used for domestic  
31  
32 201 application, of 215 L internal volume [2,31]. The refrigerator COP was kept nearly  
33  
34  
35 202 constant, varying from 0.60 to 0.61, for all engine load range investigated. The  
36  
37 203 thermodynamic simulation of each system component calculates mass, energy, entropy  
38  
39  
40 204 and exergy balances at steady state condition and neglecting pressure drop. The  
41  
42 205 exergetic efficiencies of the ammonia-water absorption refrigeration system ( ) and  
43  
44  
45 206 the system generator ( ) are calculated as [19]:  
46

47 207  
48  
49  
50  
51  
52  
53  
54 208  
55  
56

1 209  
 2  
 3  
 4 210 Where and are the total exergies of the produced cold and the engine  
 5  
 6 211 exhaust gas, respectively (kW), and is the power consumed by the solution pump  
 7  
 8  
 9 212 (kW). , , are pure ammonia specific exergies at the state 7, evaporator  
 10  
 11 213 inlet and evaporator outlet, respectively (kJ/kg), and is the exhaust gas specific  
 12  
 13  
 14 214 exergy variation from the generator inlet to outlet (kJ/kg). and are the binary  
 15  
 16 215 solution specific exergies at the states 3 and 4, respectively (kJ/kg). and are the  
 17  
 18 216 binary solution specific enthalpies at the pump inlet and outlet, respectively, in kJ/kg.  
 19  
 20  
 21 217 is the exhaust gas flow rate at the generator inlet (kg/s); and are pure  
 22  
 23 218 ammonia flow rates at the evaporator and state 7, respectively (kg/s). and are the  
 24  
 25  
 26 219 binary solution flow rates at states 3 and 4, respectively (kg/s).  
 27  
 28 220 Other results from the third stage of the simulation include component  
 29  
 30  
 31 221 irreversibilities, generator efficiency, heat transfer in the condenser, evaporator,  
 32  
 33 222 absorber and heat exchanger, pump power, COP, and the thermodynamic properties  
 34  
 35  
 36 223 used in the exergoeconomic analysis (stage 5 in Fig. 2). The exergoeconomic analysis  
 37  
 38 224 refers to the exergetic costs of system operation according to the physical structure of  
 39  
 40 225 the cogeneration system (Fig. 1), using the streams thermodynamic properties and  
 41  
 42  
 43 226 component parameters that were computed in the previous stages (Fig. 2). For the  
 44  
 45 227 exergoeconomic analysis, the unit exergetic cost at the cogeneration system inlet was  
 46  
 47  
 48 228 assumed as 1, the exergetic cost balance was applied for components and junctions, and  
 49  
 50 229 the costs distribution in the bifurcations was performed proportionally to the exergy.  
 51  
 52  
 53 230 Additionally, the negentropy was considered to be generated by dissipative equipment,  
 54  
 55 231 such as the condenser and absorber, and the exhaust gas from the diesel power generator  
 56  
 57  
 58 232 was taken as waste when assigning the costs.

Table 3 presents the fuel-product definition for each component of the cogeneration system, based on which the cogeneration plant productive structure was built (Fig. 3). Figure 3 shows that the negentropy ( ) related to heat dissipation in the condenser is located in the generator, heat exchanger, evaporator and expansion valve (streams 39 to 42), and related to heat dissipation in the absorber is located in the pressure reducing valve, generator, solution heat exchanger and solution pump (streams 35 to 38). The negentropy distribution adopted was based on the criteria that some components work with nearly pure ammonia (heat exchanger, expansion valve and evaporator) while others use ammonia-water solution (solution heat exchanger, pressure reducing valve and solution pump) or both (generator). For the generator, two negentropy streams were located (36 and 39) because it works with two fluid types: nearly pure ammonia (flow 7 in Fig. 1) and ammonia-water solution (flows 3 and 4 in Fig. 1).

The diesel engine negentropy is due to dissipation of the chemical exergy of the exhaust gas flow to the ambient (ambient product in Tab. 3 and stream 47 in Fig. 3). From the 50 streams presented in Fig. 3 and the assumptions mentioned before, 50 equations were written in the EES software to compute the unit exergetic cost for each stream, with the aim to calculate the unit exergetic cost ( , in dimensionless form) and the specific exergoeconomic cost ( ) of each stream in the productive structure. The main calculated costs were the net electrical power ( , in US\$/kW.h) and cold produced ( , in US\$/RT.h, 1 RT = 3.517 kW) by the system at the different loads and fuel replacement rates simulated. The specific costs are calculated by the following equations [19]:

1  
2  
3  
4  
5 257  
6  
7  
8  
9  
10

11 258  
12  
13

14 259 Where  $\dot{C}$  is the total stream exergetic cost (kW),  $\dot{E}$  is the total stream exergy  
15  
16 260 (kW),  $\eta$  is the exergetic efficiency (dimensionless), and  $\dot{C}_{ex}$  is the stream  
17  
18 261 exergoeconomic cost (US\$/h).  
19  
20

21 262 The exergoeconomic costs for each stream in Fig. 3 are calculated from the  
22  
23 263 exergetic unit costs. The exergoeconomic costs are due to fuel prices, taking into  
24  
25 264 account the initial investment, maintenance and external valorization. The diesel oil and  
26  
27 265 natural gas prices considered in the calculations were 0.2 US\$/L and 0.5465 US\$/m<sup>3</sup>,  
28  
29 266 respectively. These are commercialization prices for thermal power generation  
30  
31 267 established by the Brazilian Ministry of Finance [32]. The calculation of the external  
32  
33 268 valorization was based on Ref. [33], and it includes an investment cost of US\$  
34  
35 269 13,950.00 for the diesel power generator and US\$ 13,167.00 for the absorption  
36  
37 270 refrigeration system. Further details on the exergoeconomic analysis are available in  
38  
39 271 Ref. [20].  
40  
41  
42  
43  
44  
45

46 272  
47

#### 48 273 **4. RESULTS AND DISCUSSION**

49

50 274  
51  
52

53 275 Figure 4 shows that the engine exergetic efficiency increased with increasing  
54  
55 276 load power. This trend is explained because, at low loads, a high fraction of the power  
56  
57 277 produced is used to overcome friction losses. At partial load, fluid flows, mixing, heat  
58  
59  
60

1 278 transfer and combustion processes increase the specific entropy generation, thus  
2  
3 279 reducing the exergetic efficiency. It is also observed that, with increasing diesel oil  
4  
5  
6 280 replacement by natural gas at any load, the engine exergetic efficiency is enhanced due  
7  
8 281 to improved combustion. The increase of natural gas fraction in the fuel also increases  
9  
10  
11 282 the pre-mixed combustion phase, which is a process more efficient than diffusive  
12  
13 283 combustion.

14  
15  
16 284 In Fig. 5, it is observed that the exergetic efficiency of the refrigeration system  
17  
18 285 tends to decrease with increasing load, due to rise of heat transfer and irreversibility in  
19  
20 286 the refrigeration system. When the engine load increases, the exhaust gas mass flowrate  
21  
22  
23 287 and temperature are also increased (Tab. 1). Thus, more heat is transferred to the  
24  
25 288 refrigeration system, and the heat transfer process in the refrigeration system regenerator  
26  
27  
28 289 occurs with a higher temperature difference. For those reasons, both entropy generation  
29  
30 290 and irreversibility are increased, causing a decrease of the exergetic efficiency of the  
31  
32  
33 291 absorption refrigeration system. Increasing the replacement rate of diesel oil by natural  
34  
35 292 gas until 50% decreases the exhaust gas temperature (Tab. 1), which can improve the  
36  
37  
38 293 exergetic efficiency.

39  
40 294 Figure 6 shows a tendency of reducing generator exergetic efficiency when the  
41  
42 295 engine load is increased, similarly to what was observed for the absorption refrigeration  
43  
44  
45 296 system (Fig. 5). This means that the exergetic efficiency of the absorption refrigeration  
46  
47 297 system is strongly influenced by the generator exergetic efficiency. The generator  
48  
49  
50 298 exergetic efficiency decreases with increasing engine load because of higher entropy  
51  
52 299 generation (or irreversibility) caused by high heat transfer rate and temperature  
53  
54  
55 300 difference between the engine exhaust gas and the refrigeration system working fluid.

1 301 Figure 7 shows that the produced cold unit exergetic cost is increased with  
2  
3 302 increasing engine load, and is decreased with increasing replacement rate of diesel oil  
4  
5  
6 303 by natural gas. This means that more exergy is necessary to supply the refrigeration  
7  
8 304 system for each unit of produced cold when increasing engine load. In Fig. 8, it is  
9  
10  
11 305 observed that the produced power unit exergetic cost decreases for medium and high  
12  
13 306 loads while, for low and partial loads, the cost is higher. This means that less exergy is  
14  
15  
16 307 necessary to supply the engine for each unit of the produced power when increasing  
17  
18 308 engine load or, in other words, it is more interesting to operate the engine at high loads  
19  
20 309 to reduce the power generation cost. Increasing the replacement rate of diesel oil by  
21  
22  
23 310 natural gas also decreases unit exergetic cost of power generation.  
24

25 311 Figure 9 shows that the exergoeconomic cost of the cogenerated cold is  
26  
27  
28 312 increased with increasing load and decreased with increasing replacement rate of diesel  
29  
30 313 oil by natural gas. The decrease of the exergetic efficiency of the absorption  
31  
32  
33 314 refrigeration system with increasing engine load (Fig. 5) increases the irreversibility  
34  
35 315 and, thus, the final cost of the cogenerated cold. On the other hand, the exergetic  
36  
37  
38 316 efficiency of the absorption refrigeration system is increased with increasing  
39  
40 317 replacement of diesel oil by natural gas (Fig. 5), having a positive effect on the  
41  
42 318 exergoeconomic cost of the cogenerated cold (Fig. 9).  
43  
44

45 319 The variation of the exergoeconomic cost of electrical power production is  
46  
47 320 shown by Fig. 10. Unlike cold cogeneration, in this case the trend of decreasing cost  
48  
49  
50 321 with increasing load is due to the increase of the engine exergetic efficiency (Fig. 4),  
51  
52 322 which reduces the irreversibility of the power system. Increasing the replacement rate of  
53  
54  
55 323 diesel oil by natural gas increases the exergoeconomic cost of power production (Fig.  
56  
57 324 10). Considering the prices of residential rates with taxes, both the use of diesel oil as a  
58

1 325 single fuel or partially replacing it by natural gas can be competitive in the depicted  
2  
3 326 scenario if the cost of electrical power is lower than the existing rate with taxes. When  
4  
5  
6 327 natural gas is used, the exergoeconomic cost of the produced power is below the  
7  
8 328 existing rate with taxes only at intermediate and high loads. The gaseous fuel cost has a  
9  
10  
11 329 strong influence on the calculated results, playing a major role to make the cogeneration  
12  
13 330 system economically viable.

14  
15  
16 331 From comparison of the results of the present work with those when hydrogen  
17  
18 332 was used as fuel in similar conditions [19], the same trends were observed for the  
19  
20 333 produced cold and power exergoeconomic costs (Figs. 9 and 10). Nevertheless,  
21  
22  
23 334 considering the replacement rate of 50%, the reduction of the produced cold  
24  
25 335 exergoeconomic cost is of about 26% when hydrogen replaces diesel oil [19], while,  
26  
27  
28 336 using natural gas instead, the reduction is of around 17% (Fig. 9). When analyzing the  
29  
30 337 produced power exergoeconomic cost, the use of hydrogen is more viable for a slightly  
31  
32  
33 338 larger range of load power [19]. However, natural gas allows for a larger replacement  
34  
35 339 rate of diesel oil, up to 75% without major engine modification, while the maximum  
36  
37  
38 340 replacement rate of diesel oil by hydrogen was 50% [19].

## 39 341

## 42 342 **5. CONCLUSIONS**

43  
44  
45 343

46  
47 344 From the results obtained, the following conclusions can be drawn:

- 48  
49  
50 345 – Increasing engine load reduces entropy generation and irreversibility in the engine  
51  
52 346 and increases entropy generation and irreversibility in the absorption refrigeration  
53  
54  
55 347 system;



1 348 – Increasing the replacement rate of diesel oil by natural gas decreases entropy  
2  
3 349 generation and irreversibility in both the engine and the absorption refrigeration  
4  
5 350 system;  
6  
7  
8 351 – The cogeneration cold unit exergetic cost and exergoeconomic cost increase with  
9  
10 352 engine load due to an increase of exergy destruction in the absorption refrigeration  
11  
12 353 system mainly by the reduction of the exergetic efficiency in the generator of the  
13  
14 354 refrigeration system.  
15  
16 355 – The cogeneration cold unit exergetic cost and exergoeconomic cost decrease with  
17  
18 356 increasing replacement rates of diesel oil by natural gas;  
19  
20 357 – The electric power unit exergetic cost and exergoeconomic cost decrease with  
21  
22 358 increasing engine load and diesel oil replacement by natural gas rise, being viable  
23  
24 359 in the economic scenario considered if the engine is operated at medium and high  
25  
26 360 loads;  
27  
28 361 – In comparison with diesel fuel replacement by hydrogen, natural gas provides lower  
29  
30 362 decrease of the exergoeconomic cost of cold production, but allows for a larger  
31  
32 363 range of replacement rate without major engine modification.  
33  
34  
35 364

## 365 **6. ACKNOWLEDGMENTS**

366 The authors thank CAPES, ANEEL/CEMIG GT-292 research project, CNPq  
367 research project 304114/2013-8, and FAPEMIG research projects TEC PPM 0385-15  
368 and TEC BPD 0309-13 for the financial support to this work.

## 370 **7. NOMENCLATURE**

371

1	372		Specific exergoeconomic cost, US\$/kW.h or US\$/RT.h
2			
3			
4	373		Exergoeconomic cost, US\$/h
5			
6	374	CO	Carbon monoxide
7			
8	375	COP	Coefficient of Performance
9			
10			
11	376	EES	Engineering Equation Solver
12			
13	377		Specific exergy, kJ/kg
14			
15			
16	378		Total exergy, kW
17			
18	379		Total exergy cost, kW
19			
20			
21	380	h	Binary solution specific enthalpy, kJ/kg
22			
23	381		Unit exergetic cost, kW/kW
24			
25			
26	382	LiBr	Lithium Bromide
27			
28	383		Mass flowrate, kg/s
29			
30			
31	384	NG	Natural Gas
32			
33	385	NMHC	Non-Methane unburned hydrocarbons
34			
35			
36	386	NO <sub>x</sub>	Oxides of nitrogen
37			
38	387	SPECO	Specific Exergy Costing
39			
40			
41	388		Power, kW
42			
43	389		
44			
45	390		<b><i>Greek letters</i></b>
46			
47			
48	391		Variation or difference
49			
50	392		Efficiency
51			
52			
53	393		
54			
55	394		<b><i>Subscripts</i></b>
56			
57			
58	395		1, 2,... Flow number (Fig. 1) or stream number (Fig. 5)
59			
60			
61			
62			

1	396	Absorber
2		
3		
4	397	Absorption Refrigeration System
5		
6	398	Cold
7		
8	399	Chemical
9		
10		
11	400	Condenser
12		
13	401	Diesel oil
14		
15		
16	402	Diesel Engine
17		
18	403	Electric power
19		
20		
21	404	Expansion Valve
22		
23	405	Evaporator
24		
25		
26	406	Diesel oil and natural gas blend
27		
28	407	Exhaust gas
29		
30		
31	408	Generator
32		
33	409	Heat Exchanger
34		
35		
36	410	Negentropy
37		
38	411	Natural Gas
39		
40		
41	412	Pressure Reduction Valve
42		
43	413	Refrigerant
44		
45		
46	414	Shaft power
47		
48	415	Solution Heat Exchanger
49		
50		
51	416	Solution pump
52		
53	417	
54		
55		
56	418	<i>Superscripts</i>
57		
58	419	Exergetic
59		
60		
61		
62		

1 420  
2  
3 421 **8. REFERENCES**  
4  
5  
6 422  
7

- 8 423 [1] F. Táboas, M. Bourouis, M. Vallès, Analysis of ammonia/water and ammonia/salt  
9  
10 mixture absorption cycles for refrigeration purposes in fishing ships. Applied  
11 424 Thermal Engineering 66 (2014) 603-611.  
12  
13 425 <http://dx.doi.org/10.1016/j.applthermaleng.2014.02.065>  
14  
15  
16 426  
17  
18 427 [2] A. Manzela, S. Hanriot, L. Cabezas-Gómez, J. Sodr . Using engine exhaust gas  
19  
20 428 energy source for an absorption refrigeration system. Applied Energy 87 (2012)  
21  
22 1141-1148. doi:10.1016/j.apenergy.2009.07.018  
23  
24  
25 430 [3] A. Abusoglu, M. Kanoglu. Exergetic and thermoeconomic analyses of diesel engine  
26  
27 powered cogeneration: Part 1-Formulation. Applied Thermal Engineering 29  
28 431 (2009) 234-241. doi:10.1016/j.applthermaleng.2008.02.025  
29  
30  
31  
32 433 [4] O. Balli, H. Aras, A. Hepbasli. Thermodynamic and thermoeconomic analyses of a  
33  
34 trigenation (TRIGEN) system with a gas-diesel engine: Part I – Methodology.  
35 434 Energy Conversion and Management 51 (2010) 2252-2259.  
36  
37  
38 435  
39  
40 436 [5] O. Balli, H. Aras, A. Hepbasli. Thermodynamic and thermoeconomic analyses of a  
41  
42 437 trigenation (TRIGEN) system with a gas-diesel engine: Part II – An application.  
43  
44 Energy Conversion and Management 51 (2010) 2260-2271.  
45 438  
46  
47 439 doi:10.1016/j.enconman.2010.03.021  
48  
49  
50 440 [6] J. Li, S. Xu, The performance of absorption – compression hybrid refrigeration  
51  
52 441 driven by waste heat and power from coach engine, Applied Thermal Engineering  
53  
54 61 (2013) 747–755. doi:10.1016/j.applthermaleng.2013.08.048  
55 442  
56  
57  
58  
59  
60  
61  
62  
63  
64  
65

1 443 [7] M. Mostafavi, B. Agnew, Thermodynamic analysis of combined diesel engine and  
2  
3 444 absorption refrigeration unit-naturally aspirated diesel engine, Applied Thermal  
4  
5  
6 445 Engineering 17 (1997) 471-478. doi:10.1016/S1359-4311(96)00036-1  
7

8 446 [8] S. Jayasekara, S.K. Halamuge, A combined effect absorption chiller for enhanced  
9  
10  
11 447 performance of combined cooling heating and power system, Applied Energy, 127  
12  
13 448 (2014) 239-248. doi:10.1016/j.apenergy.2014.04.035  
14  
15

16 449 [9] T.K. Gogoi, K. Talukdar, Exergy based parametric analysis of a combined reheat  
17  
18 450 regenerative thermal power plant and water-LiBr vapor absorption refrigeration  
19  
20 451 system, Energy Conversion and Management 83 (2014) 119-132.  
21  
22  
23 452 doi:10.1016/j.enconman.2014.03.060  
24

25 453 [10] A. Sencan, Performance of ammonia-water refrigeration systems using artificial  
26  
27  
28 454 neural networks, Renew. Energy 32 (2007) 314-328.  
29  
30 455 doi:10.1016/j.renene.2006.01.003  
31  
32

33 456 [11] A. Ouadha, Y. El-Gotni, Integration of an ammonia-water absorption refrigeration  
34  
35 457 system with a marine Diesel engine: A thermodynamic study, Preced. Comput. Sci.  
36  
37  
38 458 19 (2013) 754-761.  
39

40 459 [12] S.A.M. Said, K. Spinder, M.A., El-Shaarawi, M.U. Siddiqui, F. Schmid, B.  
41  
42 460 Bierling, M.M.A. Khan, Design, construction and operation of a solar powered  
43  
44  
45 461 ammonia-water absorption refrigeration system in Saudi Arabia, International  
46  
47 462 Journal of Refrigeration, 62 (2016) 222-231. doi:10.1016/j.ifrefrig.2015.10.026  
48  
49

50 463 [13] W. Han, L. Sun, D. Zheng, H. Jin, S. Ma, X. Jing, New hybrid absorption-  
51  
52 464 compression refrigeration system based on cascade use of mid-temperature waste  
53  
54  
55 465 heat, Applied Energy 106 (2013) 383-390. doi:10.1016/j.apenergy.2013.01.067  
56

1 466 [14] A.A.V. Ochoa, J.C.C. Dutra, J.R.G. Henríquez, J. Rohati, Energetic and exergetic  
2  
3 467 study 10 RT absorption chiller integrated into a microgeneration system, Energy  
4  
5  
6 468 Conversion and Management 88 (2014) 545-553.  
7  
8 469 doi:10.1016/j.econman.2014.08.064  
9  
10  
11 470 [15] K. Talukdor, T.K. Gogoi, Exergy analysis of a combined vapor power cycle and  
12  
13 471 boiler flue gas driven double effect water-LiBr absorption refrigeration system.  
14  
15  
16 472 Energy Conversion and Management 108 (2016) 468-477.  
17  
18 473 doi:10.1016/j.econman.2015.11.020  
19  
20 474 [16] G. Farshi, S. Mahmoudi, M. Rosen, M. Yari, M. Amidpo, Exergoeconomic  
21  
22  
23 475 analysis of double effect absorption refrigeration systems, Energy Conversion and  
24  
25 476 Management 65 (2013) 13-25. doi:10.1016/j.enconman.2012.07.019  
26  
27  
28 477 [17] G. Farshi, S.M.S. Mahmoudi, M.A. Rosen, Exergoeconomic comparison of double  
29  
30 478 effect and combined ejector-double effect absorption systems, Applied Energy 103  
31  
32  
33 479 (2013) 700-711. doi:10.1016/j.apenergy.2012.11.022  
34  
35 480 [18] F.R. Siddiqui, M.A.I. El-Shaarawi, S.A.M. Said, Exergo-economic analysis of a  
36  
37  
38 481 solar driven hybrid storage absorption refrigeration cycle, Energy Conversion and  
39  
40 482 Management 80 (2014) 165-172. doi:10.1016/j.econman.2014.01.029  
41  
42 483 [19] M.D.M. Herrera, F.R.P. Arrieta, J.R. Sodr , Thermo-economic assessment of an  
43  
44  
45 484 absorption refrigeration and hydrogen-fueled diesel power generator cogeneration  
46  
47 485 system, International Journal of Hydrogen Energy 39 (2014) 4590-4599.  
48  
49  
50 486 doi:10.1016/j.ijhydene.2014.01.028  
51  
52 487 [20] M. Justino, M. Morais, A. Oliveira, O.S. Valente, J.R. Sodr , Fuel consumption of  
53  
54  
55 488 a diesel engine fueled with hydrogen, natural gas and diesel blends. SAE Technical  
56  
57 489 Paper 2012; 2012-36-0107:1-6.  
58

- 1 490 [21] R. Papagiannakis, D. Hountalas, Combustion and exhaust emission characteristics  
2  
3 491 of a dual fuel compression ignition engine operated with pilot Diesel fuel and  
4  
5  
6 492 natural gas, *Energy Conversion and Management* 45 (2010) 2971–2987.  
7  
8 493 doi:10.1016/j.enconman.2004.01.013  
9  
10  
11 494 [22] M. Karabektas, G. Ergen, M. Hosoz, The effects of using diethylether as additive  
12  
13 495 on the performance and emissions of a diesel engine fueled with CNG, *Fuel* 115  
14  
15  
16 496 (2014) 855–860. doi:10.1016/j.fuel.2012.12.062  
17  
18 497 [23] R. Papagiannakis, P. Kotsiopoulos, T. Zannis, E. Yfantis, D. Hountalas, C.  
19  
20 498 Rakopoulos, Theoretical study of the effects of engine parameters on performance  
21  
22  
23 499 and emissions of a pilot ignited natural gas diesel engine, *Energy* 35 (2010) 1129–  
24  
25 500 1138. doi:10.1016/j.energy.2009.06.006  
26  
27  
28 501 [24] N. Mustafi, R. Raine, S. Verhelst, Combustion and emissions characteristic of a  
29  
30 502 dual fuel engine operated on alternative gaseous fuels, *Fuel* 109 (2013) 669–678.  
31  
32  
33 503 doi:10.1016/j.fuel.2013.03.007  
34  
35 504 [25] S. Roy, A. K. Das, P. K. Bose, R. Banerjee, ANN metamodel assisted particle  
36  
37  
38 505 swarm optimization of the performance-emission trade off characteristics of a  
39  
40 506 single cylinder CRDI engine CNG dual-fuel operation, *Journal of Natural Gas*  
41  
42 507 *Science and Engineering* 21 (2014) 1156-1162.  
43  
44  
45 508 <http://dx.doi.org/j.jngse.2014.11.013>  
46  
47 509 [26] M. Shahraeni, S. Ahmed, K. Malek, B. Van Drimmelen, E. Kjeang, Life cycle  
48  
49  
50 510 emissions and cost transportation systems: case study on diesel and natural gas for  
51  
52 511 light duty trucks in municipal fleet operations, *Journal of Natural Gas Science and*  
53  
54  
55 512 *Engineering* 24 (2015) 26-34. <http://dx.doi.org/j.jngse.2015.03.009>

1 513 [27] J. Li, B. Wu, G. Mao, Research on the performance and emission characteristics of  
2 514 the LNG-Diesel marine engine, *Journal of Natural Gas Science and Engineering* 27  
3 515 (2015) 945-954. <http://dx.doi.org/j.jngse.2015.09.036>  
4  
5  
6  
7  
8 516 [28] M. Mikulski, S. Wierzbicki, Numerical investigation of the impact of gas  
9 517 composition on the combustion process in a dual-fuel compression-ignition engine,  
10 518 *Journal of Natural Gas Science and Engineering* 31 (2016) 525-537.  
11 519 <http://dx.doi.org/j.jngse.2016.03.074>  
12  
13  
14  
15  
16  
17  
18 520 [29] K. Cheenkachorn, C. Poornipatpong, G. Ho, Performance and emissions of a  
19 521 heavy-duty diesel engine fueled with diesel and LNG (liquid natural gas), *Energy*  
20 522 53 (2013) 52–57. doi:10.1016/j.energy.2013.02.027  
21  
22  
23  
24  
25 523 [30] M. Lozano, A. Valero. Calculation of exergy for substances of industrial  
26 524 interesting. Dept. of Thermodynamics and Physic – Chemistry. ETSII. Zaragoza  
27 525 University. Chemical Engineering magazine. March, 1986. (In Spanish).  
28  
29  
30  
31  
32  
33 526 [31] A. Rêgo, S. Hanriot, A. Oliveira, P. Brito, T. Rêgo. Automotive exhaust gas flow  
34 527 control for an ammonia-water absorption refrigeration system. *Applied Thermal*  
35 528 *Engineering* 64 (2014) 101-107. doi: 10.1016/j.applthermaleng.2013.12.018  
36  
37  
38  
39  
40 529 [32] Brazilian Ministry of Finance. Table of maximum retail diesel oil prices. Available  
41 530 in [www.fazenda.gov.br/portugues/legislacao /portarias\\_inter/2001/ anxport198.pdf](http://www.fazenda.gov.br/portugues/legislacao/portarias_inter/2001/anxport198.pdf).  
42 531 Accessed in November 12<sup>th</sup>, 2015.  
43  
44  
45  
46  
47 532 [33] H. Lima. Thermo-economic analysis of an absorption refrigeration system with  
48 533 LiBr-H<sub>2</sub>O pair, 3rd European Congress on Economics and Management of Energy  
49 534 in Industry, Lisbon, 2004.  
50  
51  
52  
53  
54  
55 535



1 536 **LIST OF TABLE CAPTIONS**  
2  
3  
4 537  
5  
6  
7 538 Table 1 – Experimental data from diesel power generator operating with natural gas  
8  
9 539 (NG) used in the simulation [20].  
10  
11  
12 540 Table 2 – Natural gas and diesel data assumed for calculations.  
13  
14 541 Table 3 – Fuel – Product definition by component for the productive structure.  
15  
16  
17 542  
18  
19  
20  
21  
22  
23  
24  
25  
26  
27  
28  
29  
30  
31  
32  
33  
34  
35  
36  
37  
38  
39  
40  
41  
42  
43  
44  
45  
46  
47  
48  
49  
50  
51  
52  
53  
54  
55  
56  
57  
58  
59  
60  
61  
62  
63  
64  
65

1	543	<b>LIST OF FIGURE CAPTIONS</b>
2		
3	544	
4		
5		
6	545	Figure 1 – Simplified schematics of the absorption refrigeration system coupled to the
7		
8	546	diesel power generator.
9		
10		
11	547	Figure 2 – Summary of the stages of the simulation model.
12		
13	548	Figure 3 – Cogeneration plant productive structure.
14		
15		
16	549	Figure 4 – Variation of engine exergetic efficiency with load power and natural gas
17		
18	550	concentration in the fuel.
19		
20	551	Figure 5 – Variation of absorption refrigeration system exergetic efficiency with engine
21		
22		
23	552	load power and natural gas concentration in the fuel.
24		
25	553	Figure 6 – Variation of generator exergetic efficiency with engine load power and
26		
27		
28	554	natural gas concentration in the fuel.
29		
30	555	Figure 7 – Variation of produced cold unit exergetic cost with engine load power and
31		
32		
33	556	natural gas concentration in the fuel.
34		
35	557	Figure 8 – Variation of produced power unit exergetic cost with engine load power and
36		
37		
38	558	natural gas concentration in the fuel.
39		
40	559	Figure 9 – Variation of produced cold exergoeconomic cost with engine load power and
41		
42	560	natural gas concentration in the fuel.
43		
44		
45	561	Figure 10 – Variation of produced power exergoeconomic cost with engine load power
46		
47	562	and natural gas concentration in the fuel.
48		
49		
50	563	
51		
52		

1  
2  
3  
4  
5  
6  
7  
8  
9  
10  
11  
12  
13  
14  
15  
16  
17  
18  
19  
20  
21  
22  
23  
24  
25  
26  
27  
28  
29  
30  
31  
32  
33  
34  
35  
36  
37  
38  
39  
40  
41  
42  
43  
44  
45  
46  
47  
48  
49  
50  
51  
52  
53  
54  
55  
56  
57  
58  
59  
60  
61  
62  
63  
64  
65

564  
565  
566  
567  
568

Table 1 – Experimental data from diesel power generator operating with natural gas (NG) used in the simulation [20].

		100% DIESEL OIL			75% DIESEL OIL + 25% NG			50% DIESEL OIL + 50% NG			25% DIESEL OIL + 75% NG		
ENGINE LOAD (kW)		EXHAUST GAS	DIESEL OIL	EXHAUST GAS	DIESEL OIL	NG FLOW RATE	EXHAUST GAS	DIESEL OIL	NG FLOW RATE	EXHAUST GAS	DIESEL OIL	NG FLOW RATE	
		TEMP (°C)	FLOW RATE (kg/h)	TEMP (°C)	FLOW RATE (kg/h)	(kg/h)	TEMP (°C)	FLOW RATE (kg/h)	(kg/h)	TEMP (°C)	FLOW RATE (kg/h)	(kg/h)	
0		143.01	1.91	145.00	1.86	-	138.63	1.93	-	148.41	1.32	-	
10		224.09	3.37	220.00	2.94	0.786	214.64	2.88	1.573	223.64	2.33	2.359	
20		324.17	5.17	312.00	4.50	1.171	307.11	4.10	2.341	313.99	3.48	3.511	
30		447.79	7.15	430.00	6.32	1.627	419.85	5.80	3.254	420.20	5.23	4.880	

Table 2 – Natural gas and diesel data assumed for calculations.

Natural gas		Diesel	
Component	Molar fraction	Component	Mass fraction
Nitrogen	0.015	Carbon	0.8670
Carbon Dioxide	0.007	Hydrogen	0.1271
Methane	0.871	Oxygen	0.0032
Ethane	0.078	Nitrogen	0,0000
Propane	0.029	Sulfur	0.0020
Hexane	0.000	Wet	0.0005
Hydrogen	0.000	Ash	0.0002
Lower Heating Value, kJ/kg	47451	Lower Heating Value, kJ/kg	43000
Specific exergy, kJ/kg	49243	Specific exergy, kJ/kg	42145

1 573 Table 3 – Fuel – Product definition by component for the productive structure.

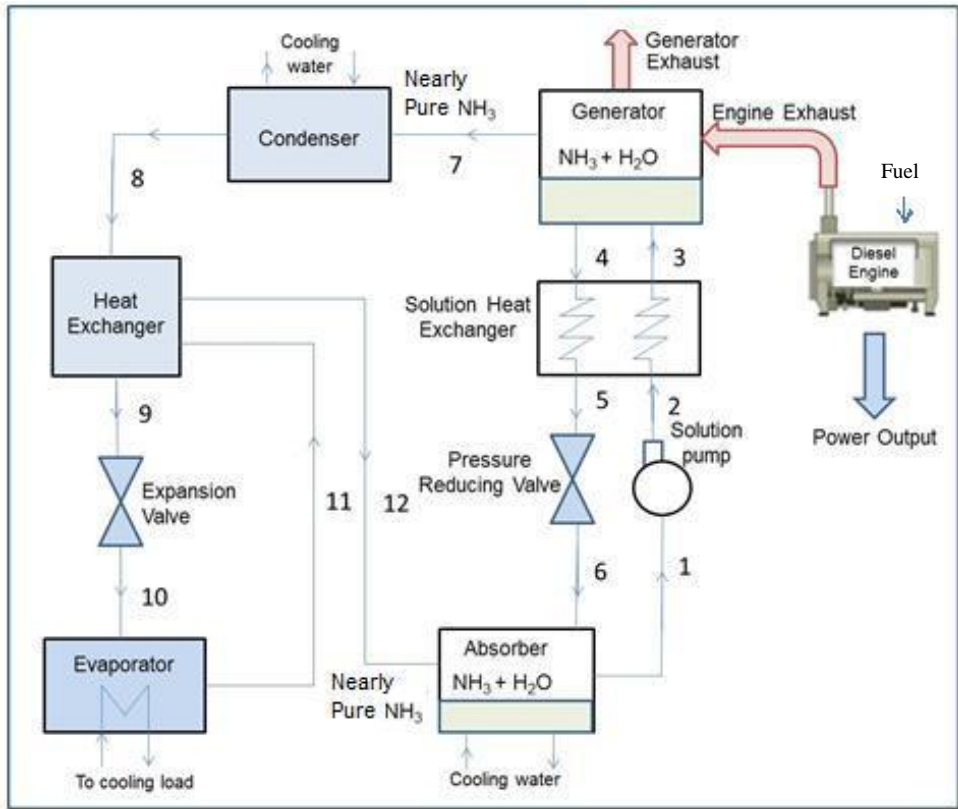
COMPONENT	FUEL	PRODUCT
Diesel engine		
Electric generator		
Ambient		
Generator		
Condenser		
Evaporator		
Absorber		
Solution pump		
Heat exchanger		
Solution heat exchanger		
Expansion valve		
Pressure reducing valve		

34 574

35  
36 575

37  
38  
39  
40  
41  
42  
43  
44  
45  
46  
47  
48  
49  
50  
51  
52  
53  
54  
55  
56  
57  
58  
59  
60  
61  
62  
63  
64  
65

1  
2  
3  
4  
5  
6  
7  
8  
9  
10  
11  
12  
13  
14  
15  
16  
17  
18  
19  
20  
21  
22  
23  
24  
25  
26  
27  
28  
29  
30  
31  
32  
33  
34  
35  
36  
37  
38  
39  
40  
41  
42  
43  
44  
45  
46  
47  
48  
49  
50  
51  
52  
53  
54  
55  
56  
57  
58  
59  
60  
61  
62  
63  
64  
65



576

577 Figure 1 – Simplified schematics of the absorption refrigeration system coupled to the  
578 diesel power generator.

579

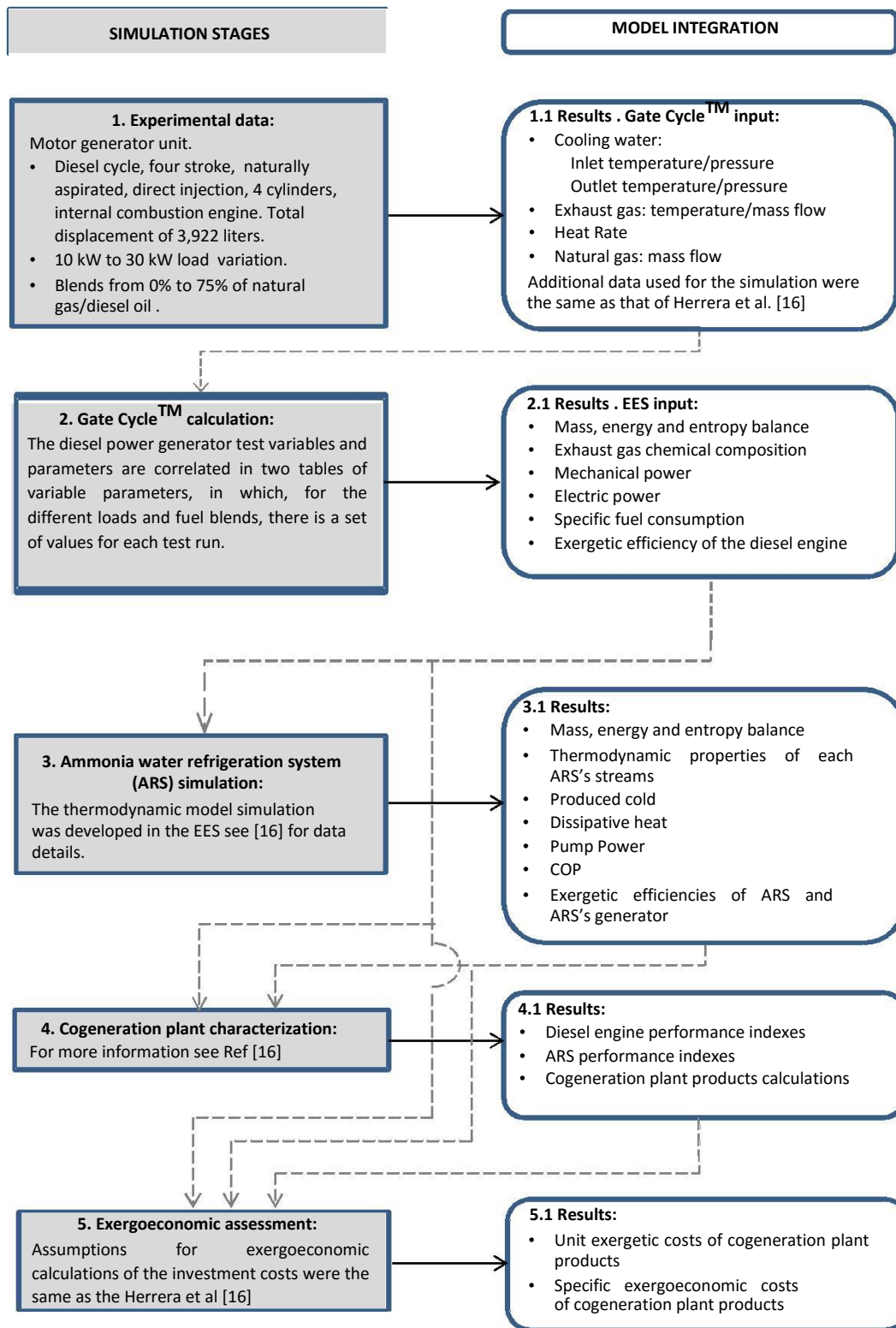


Figure 2 – Summary of the stages of the simulation model.

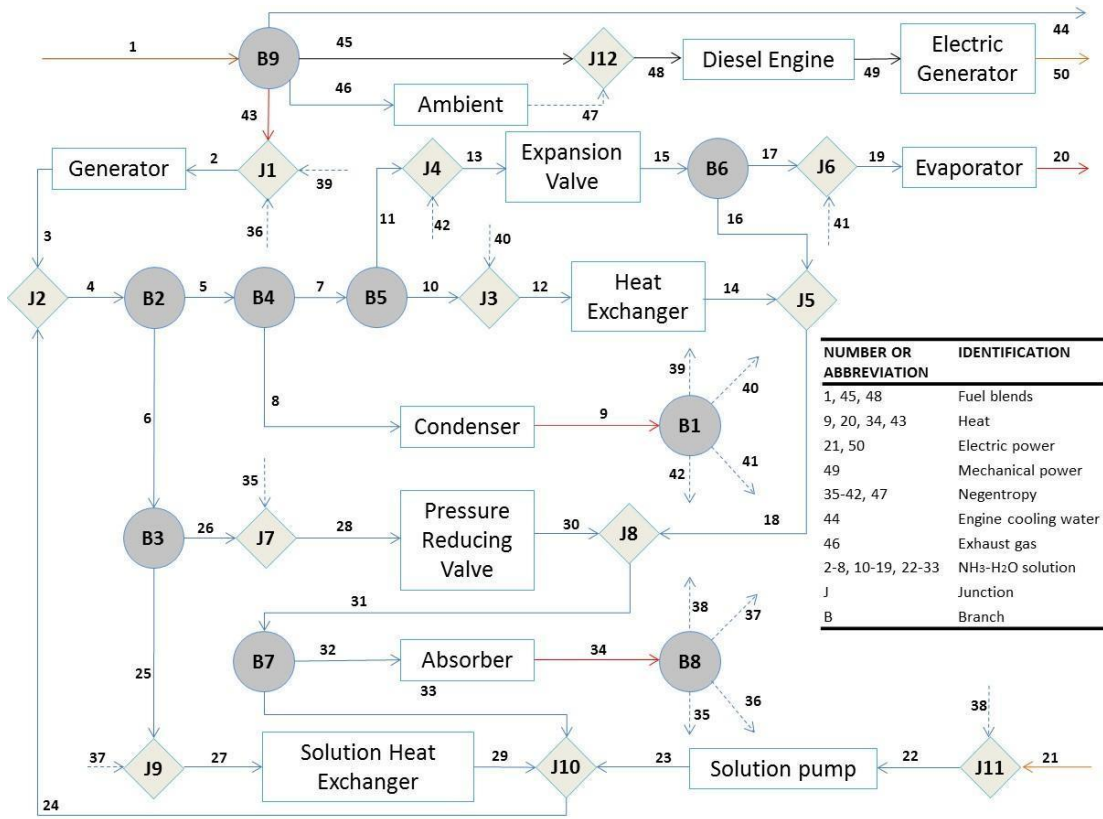
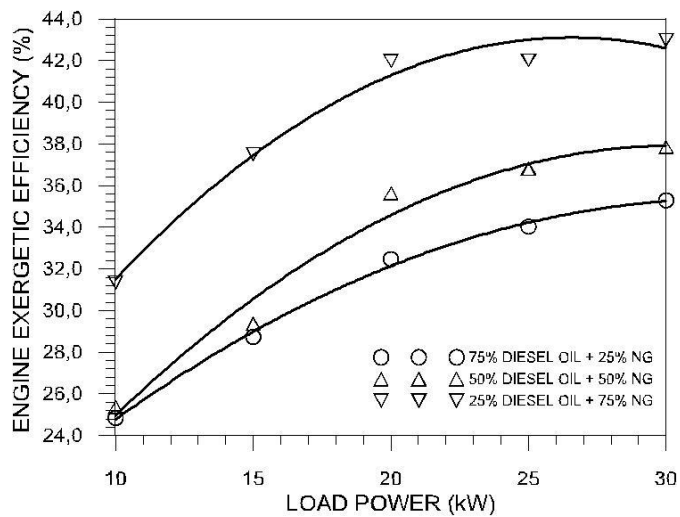


Figure 3 – Cogeneration plant productive structure.





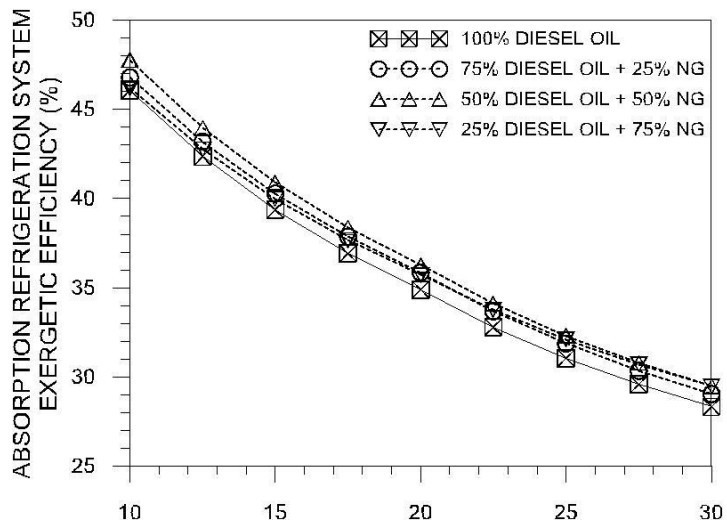
586

587

Figure 4 – Variation of engine exergetic efficiency with load power and natural gas concentration in the fuel.

588

589



590

591

Figure 5 – Variation of absorption refrigeration system exergetic efficiency with engine

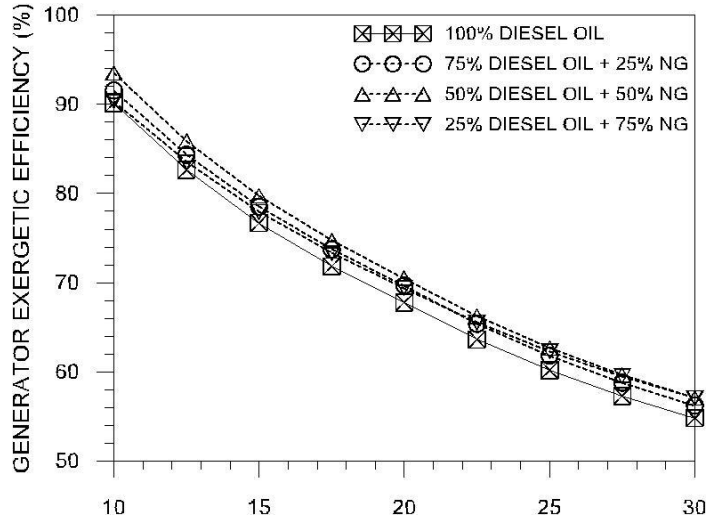
592

load power and natural gas concentration in the fuel.

593

27  
28  
29  
30  
31  
32  
33  
34  
35  
36  
37  
38  
39  
40  
41  
42  
43  
44  
45  
46  
47  
48  
49  
50  
51  
52  
53  
54  
55  
56  
57  
58  
59  
60  
61  
62  
63  
64  
65

1  
2  
3  
4  
5  
6  
7  
8  
9  
10  
11  
12  
13  
14  
15  
16  
17  
18  
19  
20  
21  
22  
23  
24  
25  
26  
27  
28  
29  
30  
31  
32  
33  
34  
35  
36  
37  
38  
39  
40  
41  
42  
43  
44  
45  
46  
47  
48  
49  
50  
51  
52  
53  
54  
55  
56  
57  
58  
59  
60  
61  
62  
63  
64  
65

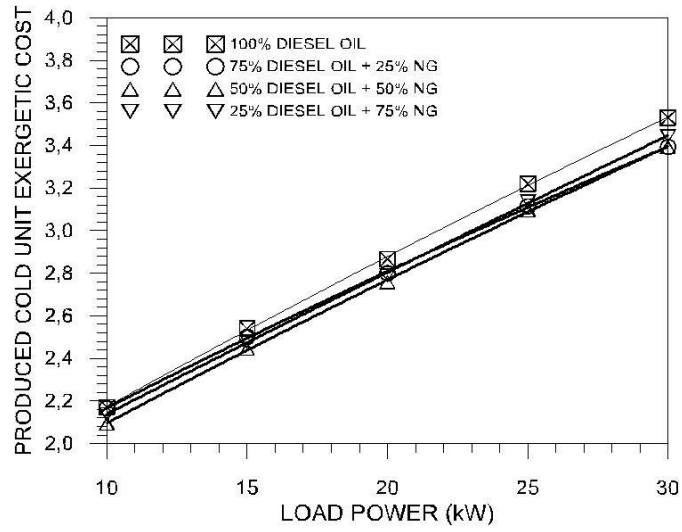


594

595 Figure 6 – Variation of generator exergetic efficiency with engine load power and  
596 natural gas concentration in the fuel.

597

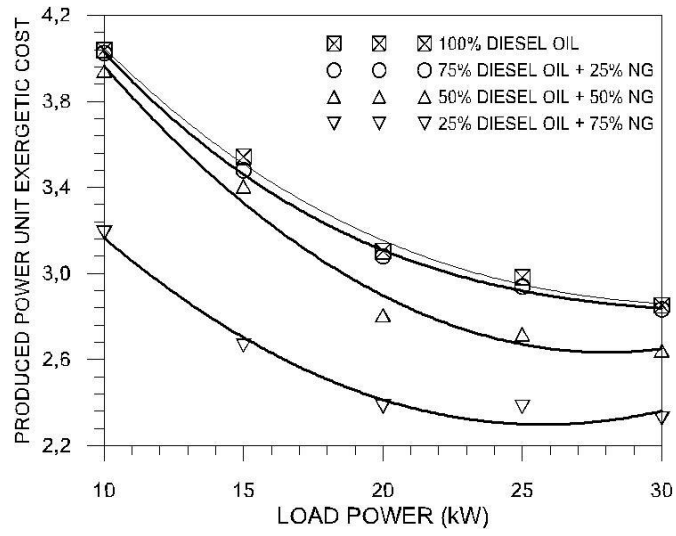
1  
2  
3  
4  
5  
6  
7  
8  
9  
10  
11  
12  
13  
14  
15  
16  
17  
18  
19  
20  
21  
22  
23  
24  
25  
26  
27  
28  
29  
30  
31  
32  
33  
34  
35  
36  
37  
38  
39  
40  
41  
42  
43  
44  
45  
46  
47  
48  
49  
50  
51  
52  
53  
54  
55  
56  
57  
58  
59  
60  
61  
62  
63  
64  
65



598

599 Figure 7 – Variation of produced cold unit exergetic cost with engine load power and  
600 natural gas concentration in the fuel.

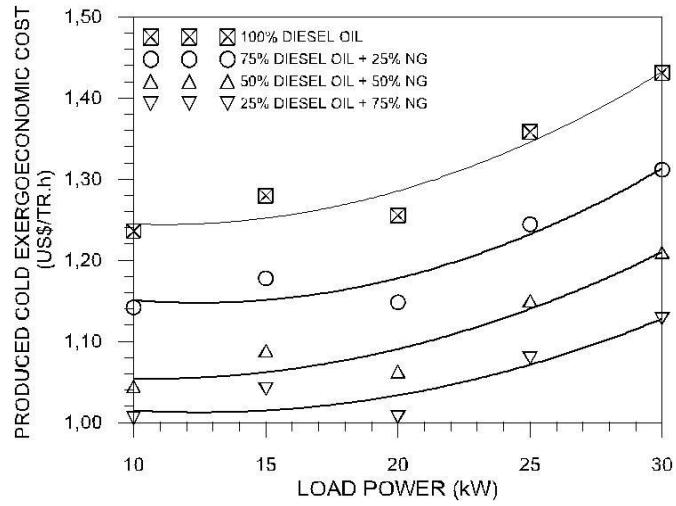
601



602

603 Figure 8 – Variation of produced power unit exergetic cost with engine load power and  
 604 natural gas concentration in the fuel.

605

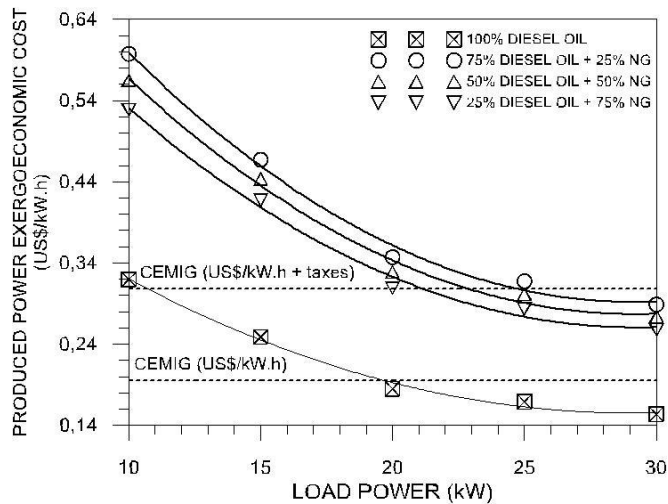


606

607 Figure 9 – Variation of produced cold exergoeconomic cost with engine load power and  
 608 natural gas concentration in the fuel.

609

25  
26  
27  
28  
29  
30  
31  
32  
33  
34  
35  
36  
37  
38  
39  
40  
41  
42  
43  
44  
45  
46  
47  
48  
49  
50  
51  
52  
53  
54  
55  
56  
57  
58  
59  
60  
61  
62  
63  
64  
65



610

611 Figure 10 – Variation of produced power exergoeconomic cost with engine load power  
 612 and natural gas concentration in the fuel.

613